Nanoscale

Accepted Manuscript

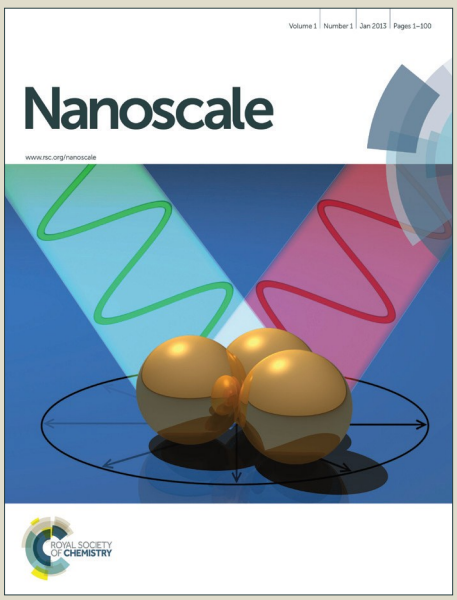

ROYAL SOCIETY OF CHEMISTRY

www.rsc.org/nanoscale

Cite this: DOI: 10.1039/c0xx00000x

www.rsc.org/xxxxxx

ARTICLE TYPE

Plasmon Coupling Enhanced Two-Photon Photoluminescence of Au@Ag Core-shell Nanoparticles and Applications in Nuclease Assay

Peiyan Yuan, Rizhao Ma, Nengyue Gao, Monalisa Garai, and Qing-Hua Xu*

Received (in XXX, XXX) Xth XXXXXXXXX 20XX, Accepted Xth XXXXXXXXX 20XX

DOI: 10.1039/b000000x

Au and Ag nanoparticles (NPs) have been known to display significantly enhanced two-photon photoluminescence (2PPL) upon formation of nanoparticle aggregates. The enhancement effects of the core-shell nanoparticles have not been explored so far. Here we have prepared Au@Ag bimetallic core-shell nanoparticles with different thicknesses (1.1, 2.1, 3.5, 4.5, and 5.5 nm) of silver coating on 19 nm Au NPs to investigate the composition effects on plasmon-coupling enhanced 2PPL. A maximum 2PPL enhancement factor ($I_{coupledNPs}/I_{isolatedNPs}$) of up to 840-fold was obtained for Au@Ag NPs with ~3.5 nm Ag nanoshells. These Au@Ag NPs were subsequently utilized in two-photon detection of S1 Nuclease as a photoluminescence turn on probe. This method displayed high sensitivity with the limit of detection of $1.4x10^{-6}$ U/μL and excellent selectivity.

Introduction

Noble metal nanoparticles (NPs) display unique optical property known as localized surface plasmon resonance (LSPR), which arises from collective oscillation of conduction band electrons.[1, 2] LSPR band strongly depends on the particle size and shape as well as plasmon coupling between metal NPs.[3-6] Plasmon coupling has drawn significant attention due to strong local electric field amplification within the gap of coupled particles, which has been utilized to enhance various optical responses such as surface-enhanced Raman scattering (SERS),[7] fluorescence,[8] two-photon photoluminescence (2PPL).[9-12] These appealing properties have found wide applications in various fields, in particular biomedical applications.[10-13]

Two-photon excitation techniques attract lots of interest because of their unique advantages such as deep penetration, less tissue auto-fluorescence, reduced photo-damage and three-dimensional confined excitation.[14, 15] These advantages can overcome the limitation of traditional one-photon techniques to allow potential in-vivo applications. Au or Ag NPs have been found to exhibit significantly enhanced 2PPL signals upon formation of nanoparticle assemblies.[9-12] Aggregation enhanced 2PPL of metal NPs has been further utilized to develop various two-photon excitation sensing and imaging applications.[10-12]

Department of Chemistry, National University of Singapore, 3 Science Drive 3, Singapore 117543

Fax: 65 67791691; Tel: 65 65162847; E-mail: chmxqh@nus.edu.sg

† Electronic Supplementary Information (ESI) available: TEM images, histograms of sizes of Au@Ag NPs; Extinction, 2PPL spectra of aggregated NPs, cysteamine, ssDNA and S1 nuclease; 2-Photon action crosee section of aggregated NPs; Lengths of ssDNA and [NaCl] effect; Excitation power dependence of 2PPL emission. See DOI: 10.1039/b000000x/.

So far up to 265-fold enhancement ($I_{coupledNPs}/I_{isolatedNPs}$) in 2PPL in Au NP solutions[12] and five order of magnitude enhancement were observed on the single particle level.[9] The enhanced 2PPL can be attributed to significantly enhanced two-photon excitation efficiency due to plasmon coupling induced further improvement in local electric field amplification as well as the resonance enhancement effects of the plasmon coupling induced LSPR band which facilitates the absorption of two photons.[9, 16]

Larger 2PPL enhancement factors help to improve the sensitivity of two-photon sensing and imaging applications and reduce the power of laser irradiation. It is important to further optimize the enhancement factors in solution. Ag NPs have been known to display more intense LSPR hence stronger local field enhancement than Au NPs. However it is difficult to prepare uniform Ag NPs in solution which requires a careful balance between pH dependent nucleation and growth processes.[17] It is relatively easier to prepare Au NPs with fine controlled size and shape.[18-20] Here we prepared a series of core-shell Au@Ag NPs with different Ag shell thicknesses. The composition effect on aggregation enhanced 2PPL has been investigated. An optimum 2PPL enhancement factor of 840-fold was obtained for Au@Ag NPs with 3.5 nm Ag shell. The large aggregation induced 2PPL enhancement of Au@Ag NPs has been further utilized to develop a two-photon sensing scheme for detection of S1 nuclease with high sensitivity and excellent selectivity.

Experimental Section

Materials and Characterizations

Gold(III) chloride trihydrate ($HAuCl_4 \cdot 3H_2O$, 99.9%), silver nitrate ($AgNO_3$, 99.9%), sodium borohydride ($NaBH_4$), and

cysteamine were purchased from Sigma-Aldrich. Trisodium citrate dehydrate (99%) was purchased from Fluka. Cetyltrimethylammonium chloride solution (CTAC, 25wt% in H_2O) and ascorbic acid were purchased from Alfa Aesar. All regents were analytical grade and used as received without further purification. All aqueous solutions were prepared in nanopure water. Ultraviolet-visible (UV-vis) extinction spectra were measured on a Hitachi UH5300 spectrophotometer. Transmission electron microscopy (TEM) images were taken on a JEOL 2010 transmission electron microscope.

Preparation of 19 nm Au NPs

19 nm Au NPs were prepared by using a three-step method modified from a previous report by Gole et al.[21] by replacing cetyltrimethylammonium bromide (CTAB) with CTAC. 3.5 nm Au NP seeds were first prepared by adding 0.3 mL of 100 mM freshly prepared ice-cold $NaBH_4$ solution into 10 mL of aqua growth solution containing $HAuCl_4$ (0.25 μM) and sodium citrate (0.25 μM). The resultant solution was vigorously shaken for 2 min and kept at room temperature for 3-5 h. 8.0 nm Au NPs were then prepared in the following step. 0.25 mL of freshly prepared 0.1 M ascorbic acid was added into the mixture of CTAC (45 mL, 0.08 M) and $HAuCl_4$ (1.125 mL, 0.01 M) solutions. 5.0 mL of 3.5 nm Au NP seed solution was then added into the resultant solution and the mixture solution was kept stirring for 10 min. In the final step, 8.0 nm Au NPs were employed as the seed to grow 19 nm Au NPs by using the same protocol. The resultant Au NPs solution was kept at room temperature for >3 h before further use. Their TEM images indicated that the obtained Au NPs were uniform with diameter of 19.0±0.9 nm (**Figure S1A&S2A**).

Preparation of Au@Ag NPs

Spherical core-shell Au@Ag NPs were prepared by using a procedure similar to a protocol that was previously used for preparation of Au@Ag nanorods.[18, 22] 10 mL of 19 nm Au NPs were first centrifuged and then washed with 0.08 M CTAC solution twice and then re-dispersed into the same volume of 0.08 M CTAC solution. 0.3 mL of 0.1 M ascorbic acid and different amounts of 10 mM $AgNO_3$ were then added into 10 ml of 19 nm Au NPs solution (0.3 nM) under magnetic stirring. The solution was heated to 60°C and maintained for 1 h. The solution changed the color from wine red to orange yellow, indicating formation of Ag shells on the surface of Au NPs to obtain Au@Ag NPs. By adjusting the amount of $AgNO_3$ solution from 25 to 200 μL, the thickness of Ag shells of Au@Ag NPs was controlled to be ~1 to 5.5 nm.

Assembly of metal NPs in solution

Cysteamine was employed as the coupling agent to induce the aggregation of metal NPs in solution. Different amounts of cysteamine stock solution were added into 2.0 mL NP solution to induce the formation of NP aggregates and were kept for 3 min at room temperature before the measurements.

Sample preparation for nuclease assay

10 mL of Au@Ag NPs (0.3 nM) was washed with 0.03% SDS three times and then re-dispersed in 1.0 mL nanopure water. 40.0 μL of 15-mer single-stranded DNA (ssDNA) (sequence: 5'-CCA ACCACACCAACC-3') solution (1×10^{-6} M), 10 μL of different amounts of S1 nuclease in stock buffer solution (10 mM CH_3COONa, 75 mM NaCl , 0.5 mM $ZnSO_4$, pH 4.6) were added into 100 μL of reaction buffer (5 times diluted from stock buffer solution). The control sample was prepared by replacing S1 Nuclease with 10 μL of stock buffer solution. After incubation at 37 °C for 30 min, 30 μL of the above mixture was added into 20μL of Au@Ag NPs solution (5.5 nM). The mixed solution was allowed to react for 30 min at room temperature (25 °C). 250 μL of 200 mM NaCl aqueous solution was added into the above mixture followed by incubation for 5 min at room temperature before the UV-vis and 2PPL measurements.

2PPL spectra measurements in solution

The excitation source for 2PPL spectra measurements is a femtosecond (fs) Ti:sapphire oscillator (Avesta TiF-100M), which gives output of 820 nm laser pulses with pulse duration of 80 fs and repetition rate of 84.5 MHz. The laser power used in the measurement was 100 mW before the sample. The laser beam was focused onto the sample by using a lens with focus length of 3 cm. To minimize the scattering from the excitation beam, an 800 nm long pass filter was placed in the excitation beam path and the emission signal was collected before passing through a pair of lenses with focus length of 3 cm and a 750 nm short pass filter at an angle of 90° to the direction of the excitation beam. A monochromator (Acton SP-2300i) coupled CCD (Princeton Instruments Pixis 100B) with an optical fibre was used to collect and detect the emission signals.

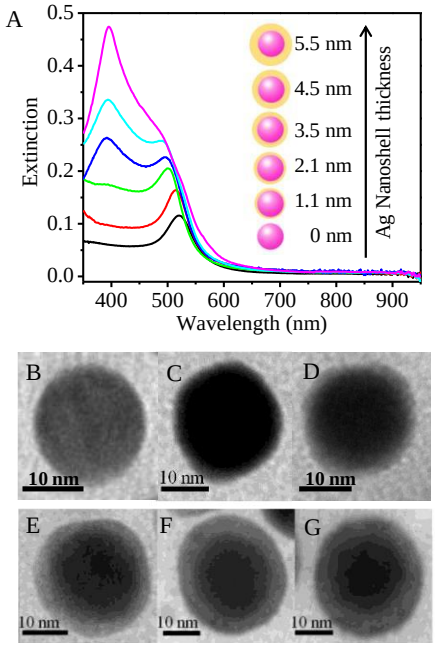

Figure 1. (A) Extinction spectra and (B-G) TEM images of Au NPs and Au@Ag NPs with different Ag shell thicknesses (1.1, 2.1, 3.5, 4.5 and 5.5 nm) in water.

Results and Discussion

Au@Ag core-shell NPs with five different Ag shell thicknesses (1.1, 2.1, 3.5, 4.5 and 5.5 nm) were prepared by using a seed-mediated growth method. 19 nm Au NPs were first prepared according to a three-step growth protocol[21] by replacing CTAB

with CTAC as the surfactant, as CTAC surfactant was known helpful in preparing core-shell NPs with well-controlled, uniform size distribution.[23-25] The obtained Au NPs were highly monodisperse with an average diameter of 19.0±0.9 nm (**Figure 1A&S2A**). Ag shells were coated onto the surface of Au NPs by reduction of $AgNO_3$ with ascorbic acid. Successful formation of Au@Ag core-shell NPs was due to closely matched crystalline lattices between Au and Ag.[24, 26, 27] Au@Ag NPs with Ag shell thicknesses of 1.1±0.2, 2.1±0.2, 3.5±0.3, 4.5±0.6, and 5.5±1.1 nm were prepared by adjusting the amount of $AgNO_3$ (**Figure 1&S2**). The CTAC surfactant can effectively protect the Ag nanoshells from oxidization. These Au@Ag NPs were found to be quite stable. The extinction and 2PPL spectra remain nearly unchanged after storage of up to three weeks (**Figure S3**). The LSPR band of 19 nm Au NPs was located at ~520 nm, which became blue-shifted after coating with Ag shells (**Figure 1**). A new LSPR band owing to the Ag shells appeared at ~391 nm, which steadily increased as the Ag shell thickness increased to 2.1 nm and above. The extinction spectra of the Au@Ag NPs match well our numerical simulation results by using the Lumerical FDTD Solutions **(Figure S4)** as well as the previously reported experimental and simulation results.[28]

Cysteamine was employed as the molecular linker to induce the coupling of Au and Au@Ag NPs as cysteamine can bind to the surface of Au and Ag NPs through its thiol and amine groups.[16, 29] Different amounts of 0.1 M cysteamine stock solution were added into 2.0 mL of Au and Au@Ag NPs solutions. Extinction spectra of all the NP solutions displayed a similar trend upon addition of cysteamine (**Figure 2 and S5**): the intensity of original LSPR bands decreased while a new LSPR band appeared at the longer wavelength region. The latter arises from formation of anisotropic assembly of Au and Au@Ag NPs, in which the longitudinally aligned dipoles give rise a strong low energy resonance.[30] Successful assembly was further confirmed by their TEM images (**Figure S1D**).

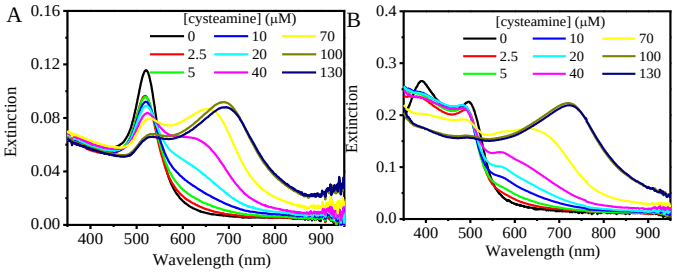

Figure 2. Extinction spectra of (A) Au NPs and (B) Au(19)@Ag(3.5) NPs before and after addition of cysteamine with different concentrations.

2PPL spectra of Au and Au@Ag NPs before and after addition of cysteamine were measured by using femtosecond laser pulses at 820 nm as the excitation source (**Figures 3 and S6**). The two-photon excitation nature of the observed photoluminescence is confirmed by the nearly quadratic excitation power dependence of the photoluminescence (**Figure S6F**). Isolated Au and Au@Ag NPs displayed very weak 2PPL due to their low emission yields and relatively small TPA cross sections.[9-12] Upon gradual addition of cysteamine to induce the formation of NPs assembly, 2PPL intensities of Au NPs and Au@Ag NPs steadily increased until reaching the optimum and then slightly decreased. The observed enhanced 2PPL signals arise from coupled metal NPs since there is no obvious two-photon excitation emission signals from cysteamine molecules even at concentration as high as 130 μM (**Figure S7**). A 2PPL enhancement factor is defined as $I_{coupledNPs}/I_{isolatedNPs}$, the ratio of 2PPL intensities after and before addition of cysteamine. The optimum 2PPL enhancement factors of all the samples were summarized in **Figure 4**. Optimum 2PPL enhancement of 840-fold was obtained for Au(19)@Ag(3.5) NPs. The mechanism for enhanced 2PPL in Au and Ag NPs has been extensively discussed before.[9-12, 16] Enhanced 2PPL can be ascribed to formation of new LSPR mode and consequently increased extinction at the excitation wavelength upon formation of NPs assemblies. These new LSPR modes act as intermediate states to facilitate absorption of two photons[9, 12, 16, 31] as well as cause larger local electric field amplification, both of which lead to enhanced two-photon excitation efficiency.[9, 12, 16, 32, 33] The local electric field can be further enhanced in the gap region due to a dynamical charge redistribution caused by the plasmon coupling.[9, 12, 16, 30]

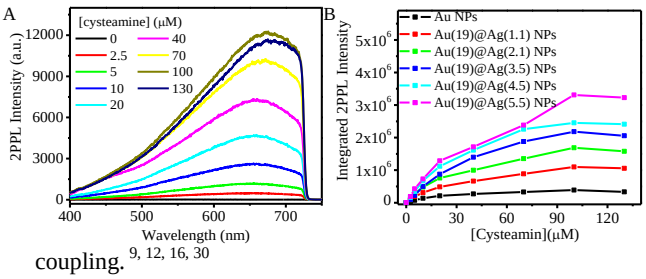

Figure 3. (A) 2PPL spectra of Au(19)@Ag(3.5) NPs, (B) Integrated 2PPL intensities of Au NPs and Au@Ag NPs with different Ag shell thicknesses after addition of cysteamine with different concentrations. Au@Ag NPs with shell thickness of 1.1, 2.1, 3.5, 4.5 and 5.5 nm.

As summarized in **Figure 4**, 2PPL intensities of both isolated and aggregated Au@Ag NPs increased with the increasing Ag shell thickness, while the optimum enhancement factor ($I_{coupledNPs}/I_{isolatedNPs}$) was observed for Au(19)@Ag(3.5) NPs. As Ag generally displays much stronger LSPR and electric field amplification compared to Au,[18] isolated and aggregated Au@Ag NPs are expected to display stronger 2PPL than the corresponding Au NPs. Au@Ag NPs with thicker Ag shells such as Au(19)@Ag(4.5) NPs and Au(19)@Ag(5.5) NPs, were less uniform in morphology and contained a small portion of nanocubes and nanorods (**Figure S1C**). As anisotropic metal NPs generally display stronger 2PPL than spherical NPs,[34] Au(19)@Ag(4.5) and Au(19)@Ag(5.5) NPs samples containing anisotropic nanostructures displayed strong 2PPL even in the isolated state, resulting in reduced enhancement factors upon the aggregate formation (**Figure 4**). The 2PPL brightness of materials is generally quantitatively characterized by two-photon action cross section, which is the product of two-photon absorption cross section and emission quantum efficiency. The two-photon action cross sections of aggregated Au and Au@Ag NPs (**Figure S8**) were calculated by using Au nanorods (48 nm × 12 nm, ϕ_{2p}= 26000 GM at 820nm) as the reference.[34] The optimum averaged two-photon action cross section the aggregated 19 nm Au NPs and Au(19)@Ag(3.5) NPs reached up to 499 GM and 2803 GM per nanoparticle, respectively.

Cite this: DOI: 10.1039/c0xx00000x
www.rsc.org/xxxxxx

ARTICLE TYPE

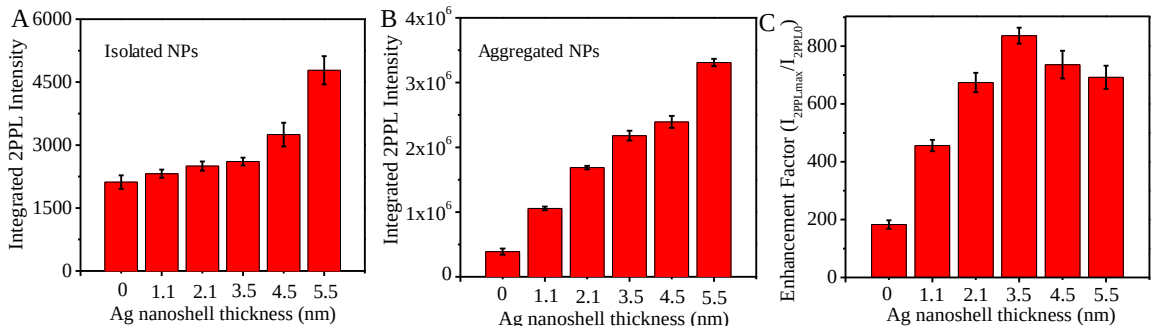

Figure 4. Integrated 2PPL intensities of Au@Ag NPs with different Ag shell thicknesses (A) before and (B) after aggregation. (C) 2PPL enhancement factors for Au@Ag NPs with different Ag shell thicknesses.

Large aggregation induced 2PPL enhancement makes these Au@Ag NPs excellent candidates for developing platform for two-photon sensing. As an illustration example, we used Au@Ag NPs as the platform for detection of S1 nuclease activity (**Figure 5A**). Nucleases are specific enzymes that possess endo- and exolytic hydrolytic activity on the phosphodiester bonds of ssDNA, producing small fragments of mono- or oligonucleotide.[35, 36] Nucleases play important roles in many biological processes such as DNA replication, recombination, repair, and gene mapping.[37-39] Various analytical methods including high performance liquid chromatography, enzyme-linked immunosorbent assay, gel electrophoresis and fluorescence,[40-45] have been utilized to detect nucleases. Most of these methods are time-consuming and need complicated experimental procedures. Furthermore, all these conventional methods are limited to in-vitro applications.

Au(19)@Ag(3.5) NPs were chosen as the platform for two-photon sensing of S1 nuclease because they gave the largest 2PPL enhancement upon assembly. This assay is based on endo- and exolytic hydrolytic activity of S1 nuclease on the phosphodiester bonds of ssDNA,[35, 36] which cleaves ssDNA strands that stabilize metal NPs to result in aggregation of metal NPs and significantly enhanced 2PPL. ssDNA can be adsorbed onto the surface of metal NPs through strong coordination interactions between the nitrogen atoms of ssDNA and the metal surfaces,[46, 47] which help to stabilize metal NPs against aggregation in solution[48, 49] The stabilizing effect of ssDNA depends on the length of ssDNA strand and long-stranded ssDNA has been known to display better stabilizing effect than shorter one.[50, 51] In the presence of S1 nuclease, long stranded ssDNA is hydrolyzed into small fragments such as mono- or oligo-nucleotides that have less stabilizing effect to metal NPs. Au@Ag NPs will consequently form aggregates, resulting in significant enhancement in 2PPL. Different 2PPL intensities could thus be utilized to detect the S1 nuclease activity.

The strand length dependent stabilizing effects of ssDNA to Au(19)@Ag(3.5) NPs in the presence of NaCl were tested by using ssDNA of different lengths (5- to 15-mer, sequences are shown in ESI). As the strand length of the stabilizing ssDNA decreased, a new LSPR band appeared at longer wavelength side of the original LSPR band of isolated Au(19)@Ag(3.5) NPs, indicating formation of NP aggregates (**Figure S9**). This result confirmed that shorter ssDNA cannot stabilize Au@Ag NPs against aggregate formation. Consequently, Au@Ag NPs in the presence of shorter ssDNA displayed much stronger 2PPL than those in the presence of long ssDNA (**Figure S9**).

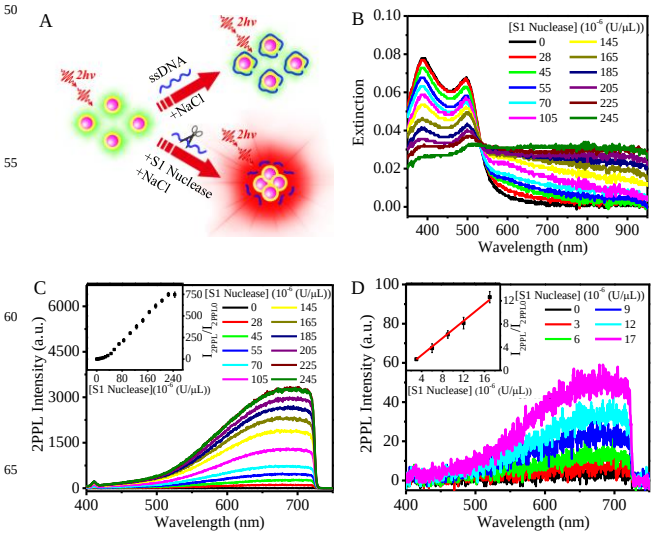

Figure 5. (A) Scheme for two-photon sensing of S1 nuclease; (B) Extinction spectra and (C, D) 2PPL spectra of Au(19)@Ag(3.5) NPs in the presence of S1 nuclease with different concentrations. Insets are plots of 2PPL enhancement factor versus S1 nuclease concentration.

The application of Au(19)@Ag(3.5) NPs in S1 nuclease assay was demonstrated by cleavage of a 15-mer ssDNA by S1 nuclease. After incubation with S1 nuclease at 37°C for 30 min, 15-mer ssDNA was hydrolyzed into fragments that cannot efficiently stabilize Au(19)@Ag(3.5) NPs. In the presence of NaCl, the Au(19)@Ag(3.5) NP solution changed the colour from yellow to blue and a new LSPR band appeared in the longer wavelength in their extinction spectra (**Figure 5B**), indicating formation of NP aggregates, which were further confirmed by

their TEM images (**Figure S10)**. The extent of aggregation was strongly dependent on the concentration of S1 nuclease. 2PPL spectra of Au(19)@Ag(3.5) NPs in the presence of different amounts of S1 nuclease were measured by using femtosecond laser pulses at 820 nm as the excitation source. In the absence of S1 nuclease, Au(19)@Ag(3.5) NPs/ssDNA exhibited very weak 2PPL signals. 2PPL intensities of the NP solution increased significantly upon addition of S1 nuclease (**Figure 5C**). As the concentration of S1 nuclease increased, 2PPL intensity steadily increased until reaching an optimum enhancement factor of ~750 fold at S1 nuclease concentration of 225x10^{-6} U/μL. The increase in 2PPL signal can be clearly observed even when nuclease was as low as 3x10^{-6} U/μL (**Figure 5D).** In this sensing experiment, the possible interference contribution of ssDNA and S1 nuclease to the observed 2PPL can be excluded as ssDNA and S1 nuclease display little emission under two-photon excitation (**Figure S11**). The enhancement in 2PPL signal is due to formation of metal NPs induced by addition of S1 nuclease. Plot of 2PPL enhancement factor versus the concentration of S1 nuclease gives a good linear relationship at the low concentration (**Figure 5D inset**). The increase in 2PPL signal can thus be utilized to quantitatively determine the concentration of S1 nuclease. This 2PPL method gives a limit of detection (LOD) of ~1.4×10^{-6} U/μL, which is lower than other reported methods (2.6×10^{-6}-7.5×10^{-3} U/μL).[40, 43, 45, 52, 53]

It needs to be noted that experimental condition needs to be optimized to prevent false positive and false negative signals. As the aggregation state of ssDNA protected metal NPs can be affected by the presence of NaCl, the concentration of NaCl is critical for the success of the scheme. When [NaCl] is too high, the ssDNA protected DNA may aggregate even in the absence of S1 nuclease to give a false positive signal or reduced sensitivity (**Figure S12A**). When [NaCl] is too low, even when the ssDNA is cleaved into short fragments, metal nanoparticles may still not form aggregates to give false negative signals (**Figure S12B**).

The specificity of this detection method has also been tested against DNase 1, RNase, and bovine serum albumin (BSA) under the same conditions. The results of both colorimetric and 2PPL selectivity tests were shown in **Figure 6**. In the presence of these agents, no obvious change in both extinction and 2PPL spectra were observed. These results indicated that this 2PPL method is not only sensitive but also selective in the detection of S1 nuclease.

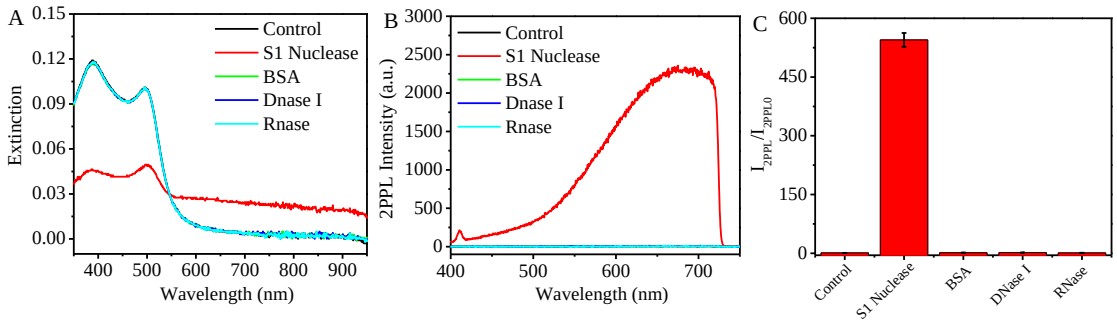

Figure 6. (A) Extinction, (B) 2PPL spectra and (C) 2PPL enhancement factor of Au(19)@Ag(3.5) NPs in the presence of S1 nuclease (165x10^{-6} U/μL), BSA (20 μg/mL), DNase 1 (1x10^{-3} U/μL) and RNase (1x10^{-3} U/μL).

Conclusion

In summary, Au@Ag core-shell nanoparticles with different Ag shell thicknesses have been prepared. 2PPL of these Au@Ag NPs became significant enhanced upon formation of NP aggregates induced by cysteamine. The optimum 2PPL enhancement factor of 840-fold was obtained for Au@Ag NPs with 3.5 nm-thick Ag nanoshell. The large aggregation induced 2PPL enhancement of Au@Ag NPs has been utilized to develop a two-photon sensing scheme for detection of S1 nuclease. This method displayed high sensitivity with a LOD of 1.4x10^{-6} U/μL and excellent selectivity. Considering the unique advantages of two-photon excitation in biological applications, this 2PPL based nuclease assay could be potentially extended to detect nucleases-related cleaving activities in-vivo.

ACKNOWLEDGMENTS

This research work was supported by the NUS AcRF Tier 1 grant (R-143-000-607-112 and R-143-000-533-112) and the National Research Foundation, Prime Minister's Office, Singapore under its Competitive Research Program (CRP Award No. NRF-CRP10-2012-04).

References

1 C. F. Bohren and D. R. Huffman, eds., *Absorption and Scattering of Light by Small Particles*, Wiley, New York, 1983.
2. S. Link and M. A. El-Sayed, *Annu. Rev. Phys. Chem.*, 2003, **54**, 331-366.
3. H. Chen, T. Ming, L. Zhao, F. Wang, L.-D. Sun, J. Wang and C.-H. Yan, *Nano today*, 2010, **5**, 494-505.
4. S. K. Ghosh and T. Pal, *Chem. Rev.*, 2007, **107**, 4797-4862.
5. O. A. Yeshchenko, I. M. Dmitruk, A. A. Alexeenko, M. Y. Losytskyy, A. V. Kotko and A. O. Pinchuk, *Phys. Rev. B*, 2009, **79**, 235438.
6. Y. B. Zheng, B. Kiraly, S. Cheunkar, T. J. Huang and P. S. Weiss, *Nano Lett.*, 2011, **11**, 2061-2065.
7. D.-K. Lim, K.-S. Jeon, H. M. Kim, J.-M. Nam and Y. D. Suh, *Nat. Mater.*, 2010, **9**, 60-67.
8. D. Cheng and Q.-H. Xu, *Chem. Commun.*, 2007, 248-250.
9. Z. Guan, N. Gao, X.-F. Jiang, P. Yuan, F. Han and Q.-H. Xu, *J. Am. Chem. Soc.*, 2013, **135**, 7272-7277.
10. C. Jiang, T. Zhao, S. Li, N. Gao and Q.-H. Xu, *ACS App. Mater. Interfaces*, 2013, **5**, 10853-10857.
11. P. Yuan, X. Ding, Z. Guan, N. Gao, R. Ma, X.-F. Jiang, Y. Y. Yang and Q.-H. Xu, *Adv. Healthcare Mater.*, 2015, **4**, 674-678.

12. P. Yuan, R. Ma, Z. Guan, N. Gao and Q.-H. Xu, *ACS App. Mater. Interfaces*, 2014, **6**, 13149-13156.
13. P. Yuan, Y. H. Lee, M. K. Gnanasammandhan, Z. Guan, Y. Zhang and Q.-H. Xu, *Nanoscale*, 2012, **4**, 5132-5137.
14. M. R. Beversluis, A. Bouhelier and L. Novotny, *Phys. Rev. B*, 2003, **68**, 115433.
15. G. S. He, L.-S. Tan, Q. Zheng and P. N. Prasad, *Chem. Rev.*, 2008, **108**, 1245-1330.
16. X.-F. Jiang, Y. Pan, C. Jiang, T. Zhao, P. Yuan, T. Venkatesan and Q.-H. Xu, *J. Phys. Chem. Lett.*, 2013, **4**, 1634-1638.
17. X. Dong, X. Ji, H. Wu, L. Zhao, J. Li and W. Yang, *J. Phys. Chem. C*, 2009, **113**, 6573-6576.
18. R. Jiang, H. Chen, L. Shao, Q. Li and J. Wang, *Adv. Mater.*, 2012, **24**, OP200-OP207.
19. O. Peña-Rodríguez and U. Pal, *Nanoscale Res. Lett.*, 2011, **6**, 1-5.
20. R. J. Stokes, A. Macaskill, P. J. Lundahl, W. E. Smith, K. Faulds and D. Graham, *Small*, 2007, **3**, 1593-1601.
21. A. Gole and C. J. Murphy, *Chem. Mater.*, 2004, **16**, 3633-3640.
22. Q. Li, R. Jiang, T. Ming, C. Fang and J. Wang, *Nanoscale*, 2012, **4**, 7070-7077.
23. C.-L. Lu, K. S. Prasad, H.-L. Wu, J.-a. A. Ho and M. H. Huang, *J. Am. Chem. Soc.*, 2010, **132**, 14546-14553.
24. Y. Ma, W. Li, E. C. Cho, Z. Li, T. Yu, J. Zeng, Z. Xie and Y. Xia, *ACS Nano*, 2010, **4**, 6725-6734.
25. M. Zayats, R. Baron, I. Popov and I. Willner, *Nano Lett.*, 2004, **5**, 21-25.
26. A. K. Samal, L. Polavarapu, S. Rodal-Cedeira, L. M. Liz-Marzán, J. Pérez-Juste, and I. Pastoriza-Santos, *Langmuir*, 2013, **29**, 15076-15082.
27. B. Liu, G. Han, Z. Zhang, R. Liu, C. Jiang, S. Wang and M.-Y. Han, *Anal. Chem.*, 2011, **84**, 255-261.
28. O. Peña-Rodríguez and U. Pal, *Nanoscale*, 2011, **3**, 3609-3612.
29. A. Abbas, L. Tian, R. Kattumenu, A. Halim and S. Singamaneni, *Chem. Commun.*, 2012, **48**, 1677-1679.
30. N. J. Halas, S. Lal, W.-S. Chang, S. Link and P. Nordlander, *Chem. Rev.*, 2011, **111**, 3913-3961.
31. P. Biagioni, M. Celebrano, M. Savoini, G. Grancini, D. Brida, S. Mátéfi-Tempfli, M. Mátéfi-Tempfli, L. Duò, B. Hecht, G. Cerullo and M. Finazzi, *Phys. Rev. B*, 2009, **80**, 045411.
32. P. Ghenuche, S. Cherukulappurath, T. H. Taminiau, N. F. van Hulst and R. Quidant, *Phys. Rev. Lett.*, 2008, **101**, 116805.
33. P. J. Schuck, D. P. Fromm, A. Sundaramurthy, G. S. Kino and W. E. Moerner, *Phys. Rev. Lett.*, 2005, **94**, 017402.
34. N. Gao, Y. Chen, L. Li, Z. Guan, T. Zhao, N. Zhou, P. Yuan, S. Q. Yao and Q.-H. Xu, *J. Phys. Chem. C*, 2014, **118**, 13904-13911.
35. F. Harada and J. E. Dahlberg, *Nucleic Acids Res.*, 1975, **2**, 865-871.
36. R. C. Wiegand, G. N. Godson and C. M. Radding, *J. Biol. Chem.*, 1975, **250**, 8848-8855.
37. S. M. Linn, R. S. Lloyd and R. J. Roberts, in *2nd edn*, Cold Spring Harbor Laboratory Press, Cold Spring Harbor, NY, 1993.
38. M. Ma, L. Benimetskaya, I. Lebedeva, J. Dignam, G. Takle and C. A. Stein, *Nat. Biotech.*, 2000, **18**, 58-61.
39. R. J. Roberts, *Nucleic Acids Res.*, 1990, **18**, 2331-2365.
40. F. Feng, Y. Tang, F. He, M. Yu, X. Duan, S. Wang, Y. Li and D. Zhu, *Adv. Mater.*, 2007, **19**, 3490-3495.
41. A. Jeltsch, A. Fritz, J. Alves, H. Wolfes and A. Pingoud, *Anal. Biochem.*, 1993, **213**, 234-240.
42. L. W. McLaughlin, F. Benseler, E. Graeser, N. Piel and S. Scholtissek, *Biochem.*, 1987, **26**, 7238-7245.
43. F. Pu, D. Hu, J. Ren, S. Wang and X. Qu, *Langmuir*, 2009, **26**, 4540-4545.
44. A. L. Rosenthal and S. A. Lacks, *Anal. Biochem.*, 1977, **80**, 76-90.
45. M. Wang, D. Zhang, G. Zhang, Y. Tang, S. Wang and D. Zhu, *Anal. Chem.*, 2008, **80**, 6443-6448.
46. H. Li and L. Rothberg, *Proc. Natl. Aca. Sci. U.S.A.*, 2004, **101**, 14036-14039.
47. H. Li and L. Rothberg, *J. Am. Chem. Soc.*, 2004, **126**, 10958-10961.
48. J. Wang, L. Wang, X. Liu, Z. Liang, S. Song, W. Li, G. Li and C. Fan, *Adv.Mater.*, 2007, **19**, 3943-3946.
49. L. Wang, X. Liu, X. Hu, S. Song and C. Fan, *Chem. Commun.*, 2006, 3780-3782.
50. A. B. Steel, R. L. Levicky, T. M. Herne and M. J. Tarlov, *Biophys. J.*, 2000, **79**, 975-981.
51. X. Zhang, M. R. Servos and J. Liu, *Langmuir*, 2012, **28**, 3896-3902.
52. R. Cao, B. Li, Y. Zhang and Z. Zhang, *Chem. Commun.*, 2011, **47**, 12301-12303.
53. Y. Xiao, F. Shu, K.-Y. Wong and Z. Liu, *Anal. Chem.*, 2013, **85**, 8493-8497.

TOC: